



DFT-Based Chemical Reactivity Descriptors, Pharmacokinetics and Molecular Docking Studies of Thymidine Derivatives

Mohammad Ahad Hossain¹, Shahin Sultana¹, Mohammad Mazherul Islam¹, Sonia Akhter¹, Faria Nur¹, Fatima Majabin¹, Kantom Islam¹, Kazi Jawad Hossain¹, Yasuhiro Ozeki² , Sarkar M. A. Kawsar^{1*} 

¹Laboratory of Carbohydrate and Nucleoside Chemistry (LCNC), Department of Chemistry, Faculty of Science, University of Chittagong, Bangladesh

²Graduate School of NanoBio Sciences, Yokohama City University, Yokohama, Japan

Email: *akawsarabe@yahoo.com

How to cite this paper: Hossain, Md.A., Sultana, S., Islam, Md.M., Akhter, S., Nur, F., Majabin, F., Islam, K., Hossain, K.J., Ozeki, Y. and Kawsar, S.M.A. (2023) DFT-Based Chemical Reactivity Descriptors, Pharmacokinetics and Molecular Docking Studies of Thymidine Derivatives. *Computational Chemistry*, 11, 81-103.

<https://doi.org/10.4236/cc.2023.114006>

Received: September 7, 2023

Accepted: October 28, 2023

Published: October 31, 2023

Copyright © 2023 by author(s) and Scientific Research Publishing Inc.

This work is licensed under the Creative Commons Attribution International License (CC BY 4.0).

<http://creativecommons.org/licenses/by/4.0/>



Open Access

Abstract

Thymidine-containing derivatives are considered to be among the most significant derivatives in medicinal chemistry. In this study, we employed a combined computational approach involving density-functional theory (DFT) calculations, molecular docking simulations, and absorption, distribution, metabolism, excretion, and toxicity (ADMET) property predictions. Prediction of activity spectra for substances (PASS) revealed promising antiviral, antimicrobial and anti-carcinogenic activities of these thymidine derivatives. Using Gaussian 09, we optimized the molecular structures of the thymidine derivatives to obtain their stable conformations and calculate their electronic properties. Subsequently, molecular docking simulations were performed to explore the binding interactions between the thymidine derivatives and the active site of the *Candida albicans* (PDB: 1IYL and 2Y7L) proteins. The docking results were evaluated based on docking scores, hydrogen bonding, and hydrophobic interactions and revealed favorable binding interactions between the thymidine derivatives and the proteins, suggesting their potential as antifungal agents. The thermodynamic properties, including binding free energy, enthalpy, and entropy changes were determined to assess the stability and strength of the ligands-protein complexes. The calculated pharmacokinetic parameters, such as ADMET properties, provided insights into the drug-likeness and potential bioavailability of the thymidine derivatives. These results offer a foundation for further experimental investigations and the design of novel antifungal agents targeting *Candida albicans* infections.

Keywords

Thymidine, DFT, Molecular Docking, Pharmacokinetics, *Candida albicans*

1. Introduction

Nucleoside agents (NAs) are the fundamental structural elements of DNA and RNA, comprising a sugar moiety connected to a nitrogen base through an N-glycosidic bond. It is interesting to note that a nucleoside's sugar moiety may be readily modified by adding various heteroatoms and substituents, among other things, to change the nucleoside's biological activity and its chemical and physical characteristics [1]. Recently, several medications used to treat infectious disorders caused by HIV, hepatitis B or C, and herpes viruses have been developed around nucleoside derivatives [2]. Additionally, due to their antiviral and anticancer properties, nucleoside derivatives have enormous therapeutic significance as pharmaceuticals [3].

Nucleoside analogs often exhibit antiviral efficacy by preventing viral replication by preventing cell division, impairing DNA/RNA synthesis, or decreasing the function of cellular or viral enzymes. The nucleoside analogs entecavir (an HIV/AIDS and hepatitis B inhibitor), telbivudine (a hepatitis B inhibitor), clevudine (a hepatitis B inhibitor), stavudine (an HIV/AIDS inhibitor), zalcitabine (a reverse transcriptase inhibitor), lamivudine (a first-generation nucleoside reverse transcriptase inhibitor), cordycepin (an inhibitor of RNA synthesis), and cordycepin triphosphate (a polyadenylation inhibitor, antineoplastic, antioxidant, and anti-inflammatory drug) have been used to treat various viral illnesses. For treating a variety of viral illnesses, including Ebola, dengue, and Zika, they have been the preferred drugs [4]. A number of members of the Enterobacteriaceae family, including strains of *Escherichia coli*, *Salmonella typhimurium*, *Klebsiella pneumoniae*, *Shigella flexneri*, and *Enterobacter aerogenes*, are highly susceptible to the thymidine analog 3'-azido-3'-deoxythymidine (AZT). Additionally, AZT was bactericidal to *Vibrio cholerae* and *Vibrio anguillarum*, a fish disease. *Pseudomonas aeruginosa*, gram-positive bacteria, anaerobic bacteria, *Mycobacterium tuberculosis*, nontuberculous mycobacteria, and a wide variety of fungal pathogens were unaffected by AZT. 2',3'-Dideoxyadenosine and 9- β -D-arabinofuranosyladenine are two potent nucleoside inhibitors of bacteria [5]. The sugar moiety, also known as ribofuranose or deoxyribofuranose of nucleosides, can be modified by adding heteroatoms, changing the sugar substituents, changing the oxygen position inside the sugar ring, changing the ring size or switching out the sugar moiety entirely [6]-[13]. According to their unique chemical and physical characteristics, these modifications might result in dramatic differences in biological activity and the level of selective toxicity [14] [15] [16] [17] [18]. Thymidine analogs and nucleobases are a pharmacologically varied class that contains cytotoxic substances, antibacterial agents, and immuno-

suppressive chemicals, according to some recent studies [19]-[26]. In most cases, the direct method [27] [28] resulted in larger yields at less cost. However, a sizeable number of pyrimidine and purine derivatives that have undergone clinical approval, such as those that have been halogenated, azolated, and acylated, have been demonstrated to have antibacterial action. In this study, we concentrated on computational analyses of previously synthesized thymidine and its derivatives. The thermal, electrical, and biological properties of the compounds were evaluated using *in silico* techniques. Using the basis set 6 - 31 G (d, p) and the B3LYP method, the thermodynamic and electrical characteristics and molecular docking are predicted for the first time.

2. Computational Method

2.1. Software Used

In the current investigation, the following software systems were employed: 1) Gaussian 09; 2) Gausssum 3.0; 3) PyRx 0.8; 4) 4.2.6 Swiss-Pdb 4.1.0; 5) Discovery Studio 3.5; 6) PyMOL 2.3; 7) Hyperchem-8.0.1; 8) ChemDraw-21.0.

2.2. Optimization and Chemical Reactivity Descriptors

Gaussian 09 software was used in this investigation to analyze a number of compounds [29]. GaussView 6 was used to draw the structures. The first stage in obtaining the leading characteristic parameters of the compounds is to optimize the molecular structure to obtain a configuration that is characterized by minimal free energy using DFT and the B3LYP technique using a basis set 6 - 31 G (d,p) and to optimize and predict their thermal and molecular orbital properties. In Gaussian 09, the convergence criteria refer to the conditions that determine when the geometry optimization process is considered complete. These criteria help ensure that the optimization has reached a stable and energetically favorable configuration. In our calculation, the convergence criteria included the maximum force, RMS force, maximum displacement, RMS displacement and energy change.

Density functional theory (DFT) serves as a supplementary approach to wavefunction-based methods such as Hartree-Fock (HF) and post-HF methods involving electron correlation. While wavefunction-based methods can yield accurate results, they share a common drawback related to computational time and cost. This limitation arises from the necessity to calculate two-electron integrals over molecular orbitals, with a scaling that increases with the number of basis functions denoted as K . For instance, HF scales as K^4 , a practical value often approximated to $K^{2.5}$ in practice, and MP2 and CID exhibit scaling as K^5 . In contrast, DFT has gained significant attention due to its reduced computational time, comparable accuracy, and efficiency in handling large molecular systems. “Becke, 3-parameter, Lee-Yang-Parr” or B3LYP for short, is the most widely used density functional theory (DFT) approach. It is well known for its accuracy in predicting molecular structures and various thermochemical properties [30].

The 6-31G basis set belongs to the Pople family of valence double-zeta basis sets. where “6” indicates that the core orbitals are described using 6 Gaussian functions (GTO), and “31” the valence orbitals are divided into two components using the 3 GTO + 1 GTO. The (d,p) are polarization functions, such as introducing a 1p orbital to hydrogen or 2d to carbon.

The dipole moment, enthalpy, free energy, and electrical energy were calculated for all the analogs. Following optimization, these structures were employed for molecular docking, molecular reactivity descriptors, and ADMET predictions. Numerous calculation methods in acceptable forms were utilized to obtain the values of chemical reactivity and associated descriptors [31] [32]. Frontier molecular orbital features, HOMO (highest occupied molecular orbital) and LUMO (lowest unoccupied molecular orbital) were counted at the same level of theory. For each of the thymidine analogs, the HOMO-LUMO energy gap, hardness (η), and softness (S) were calculated from the energies of the frontier HOMO and LUMO as reported, considering Parr and Pearson’s interpretation of DFT and Koopman’s theorem [33] [34] on the correlation of chemical potential (μ), electronegativity (χ) and electrophilicity (ω) with HOMO and LUMO energy (ε). The following equations were used to calculate global chemical reactivity by analyzing molecular orbital features.

$$\begin{aligned} \text{Gap } (\Delta\varepsilon) &= \varepsilon\text{LUMO} - \varepsilon\text{HOMO} & \mu &= \frac{[\varepsilon\text{LUMO} + \varepsilon\text{HOMO}]}{2} \\ \eta &= \frac{[\varepsilon\text{LUMO} - \varepsilon\text{HOMO}]}{2} & \chi &= -\frac{[\varepsilon\text{LUMO} + \varepsilon\text{HOMO}]}{2} \\ S &= \frac{1}{\eta} & \omega &= \frac{\mu^2}{2\eta} \end{aligned}$$

2.3. PASS Prediction

A wide range of biological processes were predicted using web-based PASS (prediction of activity spectra for drugs;

<http://www.pharmaexpert.ru/PASSonline/index.php>). This technology was developed to predict a wide variety of biological processes with 90% accuracy [35] [36] [37]. The structures were created by using ChemDraw 21.0 and then saved in Smiles format before being used to predict the biological spectrum using the PASS online version. Pa (probability for active compound) and Pi (probability for inactive compound) were used to represent the outcome. In this case, Pa > Pi is taken into account on a scale of 0.000 to 1.000, and often, Pa + Pi = 1. The PASS prediction results were interpreted and used in a flexible manner, such as 1) when Pa > 0.7, the chance to find the activity experimentally is high; 2) if 0.5 < Pa < 0.7, the chance to find the activity experimentally is less, but the compound is probably not so similar to known pharmaceutical agents; 3) if Pa < 0.5, the chance to find the activity experimentally is less but not the chance to find structurally [38]. As a result, the projected activity of the spectrum is referred to as the compound’s intrinsic attribute.

2.4. Protein Preparation and Molecular Docking

(PDB: 1IYL and 2Y7L), which were recovered from the protein data bank at <http://www.ecsb.org>, identified several *C. albicans* proteins in their crystal 3D structure. To create the raw protein strain for molecular docking, the water molecules and additional ligands that had been connected to the protein before were removed using the PYMOL program (Version: 2.5.3). After that, the proteins were subjected to energy reduction using Swiss-Pdb Viewer (version 4.1.0). Proteins (macromolecules) and ligands were opened in PyRx. After energy reduction, the ligands were converted to PDBQT format. The protein and ligands were submitted to the Vina wizard for docking, and the grid box was maintained at 54.8087, 56.2807 and 67.6774 Å for 1IYL and 42.8078, 76.8638 and 52.5086 Å for 2Y7L along the X, Y, and Z axes, respectively. The generated file was saved and studied further with BIOVIA Discovery Studio [18] [39].

2.5. ADMET and Prediction of Drug-Likeness Parameters

In computational chemistry, computer simulation is used to help solve chemical problems. It computes the physicochemical characteristics of produced compounds using theoretical chemistry methodologies incorporating inefficient computer algorithms. It can predict molecular energies and structures, transition state structures, bond and reaction energies, molecular orbitals in different solvent phases, vibrational frequencies, thermochemical properties, reaction pathways, spectroscopic quantities, and many other molecular properties for systems in the solid, gas, or solution phase. ADMET is a computer program that estimates the pharmacokinetic characteristics and qualities of drug-like compounds based on their molecular structures [40]. The SwissADME web tool (<http://www.swissadme.ch>) is free software that predicts the physicochemical qualities, absorption, distribution, metabolism, elimination, and pharmacokinetic properties of molecules, all of which are important factors for future clinical trials. It takes into account six important physicochemical properties: lipophilicity, flexibility, solubility, and size. This research may be utilized to establish a starting point for laboratory synthesis as well as to help in understanding experimental results.

3. Results and Discussion

3.1. PASS Prediction

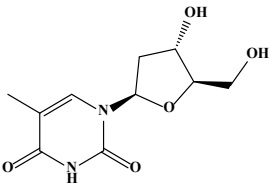
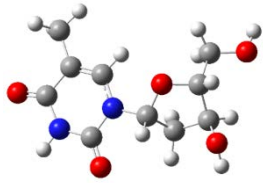
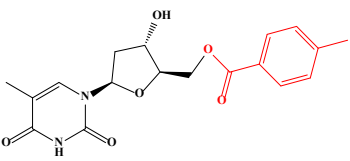
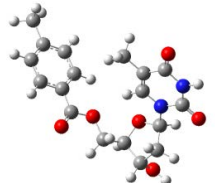
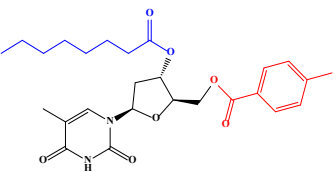
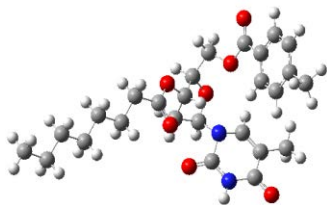
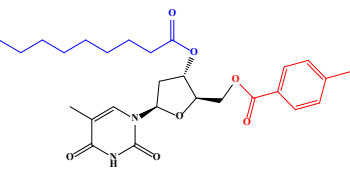
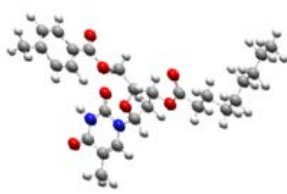
It seems that a large number of research projects have not reached the final stage because severe unfavorable side effects and toxicity are unknown, and these unfavorable effects are found or arise far too late. However, today, in this modern age, it is possible to predict more than 3678 pharmacological effects, modes of action, carcinogenicity, teratogenicity, and other biological properties of compounds using an easy online server named PASS Online. PASS results in their designated Pa and Pi forms are presented in **Table 1**. PASS prediction of compounds 1-7 was found to be $0.679 < Pa < 0.906$ antiviral, $0.583 < Pa < 0.852$ an-

timicrobial and $0.645 < Pa < 0.806$ anticarcinogenic [41] [42] [43]. This indicated that the compounds were more potent against antiviral activity than against bacterial and anti-carcinogenic activity. The optimized structures of the compounds are displayed in **Table 2**, where all compounds were fully converged.

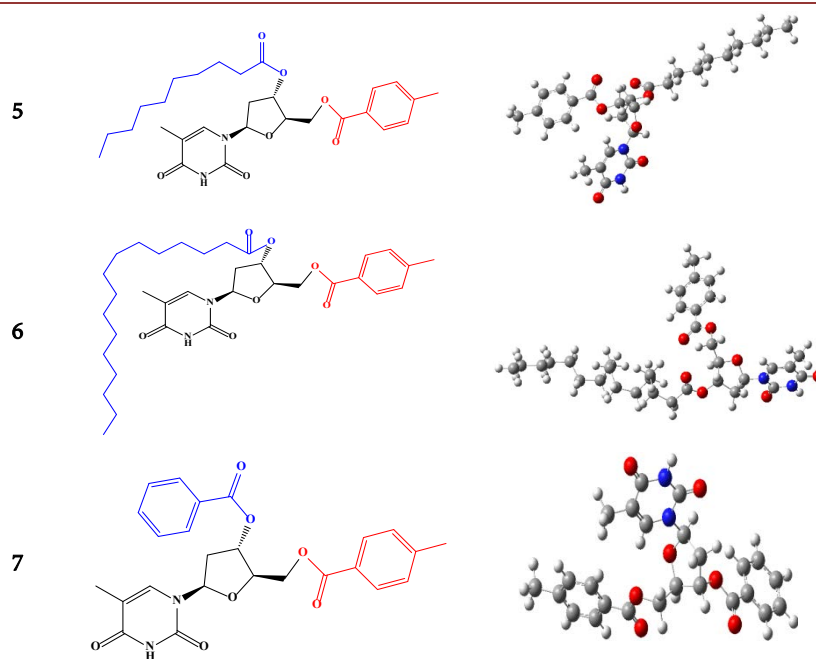
Table 1. Predicted biological activities of the thymidine derivatives using PASS software.

| Entry | Antiviral | | Antimicrobial | | Anti-carcinogenic | |
|-------|-----------|-------|---------------|-------|-------------------|-------|
| | Pa | Pi | Pa | Pi | Pa | Pi |
| 1 | 0.906 | 0.002 | 0.852 | 0.003 | 0.806 | 0.005 |
| 2 | 0.774 | 0.004 | 0.664 | 0.059 | 0.719 | 0.008 |
| 3 | 0.680 | 0.003 | 0.716 | 0.040 | 0.699 | 0.009 |
| 4 | 0.680 | 0.003 | 0.716 | 0.040 | 0.699 | 0.009 |
| 5 | 0.679 | 0.008 | 0.669 | 0.031 | 0.645 | 0.034 |
| 6 | 0.680 | 0.003 | 0.716 | 0.040 | 0.699 | 0.009 |
| 7 | 0.696 | 0.004 | 0.583 | 0.094 | 0.689 | 0.009 |

Table 2. Chemical and optimized structure of thymidine (1) and its derivatives (2 - 7).

| Entry | Structure | Optimized |
|-------|--|---|
| 1 |  |  |
| 2 |  |  |
| 3 |  |  |
| 4 |  |  |

Continued



3.2. Thermodynamic Analysis

Usually, alterations in molecular structure significantly influence structural properties, including thermal and molecular orbital parameters. The spontaneous reaction and stability of a product can be elucidated from the free energy and enthalpy values (**Table 3**) [44] [45] [46].

Highly negative values are more suitable for thermal stability. In drug design, hydrogen bond formation and nonbonded interactions are also influenced by the dipole moment. A higher dipole moment can improve the binding property [47] [48]. The free energy of thymidine is -874.9462 Hartree, whereas the Gibbs free energy of derivative **6** is -1961.2611 Hartree, respectively. The highest electronic energy was observed for **6** (-1961.9761 Hartree), and the highest dipole moment was observed for **5** (9.4399 Debye). The presence of a bulky acylating group suggests the possible improvement of the polarity of derivative **6**, which shows the highest polarity value of 398.7220 a.u.

3.3. Frontier Molecular Orbital Analysis

The frontier molecular orbitals are the most important orbitals in a molecule, and they are considered to characterize the chemical reactivity and kinetic stability. These frontier molecular orbitals are known as the highest occupied molecular orbital (HOMO) and the lowest unoccupied molecular orbital (LUMO) (**Table 4**).

Table 4 represents the values of orbital energies, along with the two global chemical descriptors, hardness and softness, which are also calculated for all compounds. The highest softness was observed for compound **4**. Compound **6**

Table 3. Thermodynamic properties of thymidine (1) and its derivatives (2 - 7).

| Compound | Stoichiometry | Electronic Energy | Enthalpy | Gibbs free Energy | Dipole moment | Polarizability |
|----------|---|-------------------|------------|-------------------|---------------|----------------|
| 1 | C ₁₀ H ₁₄ N ₂ O ₅ | -875.1508 | -874.8839 | -874.9463 | 4.9214 | 132.0463 |
| 2 | C ₁₈ H ₂₀ N ₂ O ₆ | -1258.8862 | -1258.4924 | -1258.5764 | 3.8849 | 217.8913 |
| 3 | C ₂₆ H ₃₄ N ₂ O ₇ | -1647.4569 | -1646.8425 | -1646.9548 | 4.7339 | 307.0927 |
| 4 | C ₂₇ H ₃₆ N ₂ O ₇ | -1686.7689 | -1686.1245 | -1686.2407 | 5.8310 | 322.4273 |
| 5 | C ₂₈ H ₃₈ N ₂ O ₇ | -1726.0754 | -1725.4015 | -1725.5206 | 9.4399 | 333.6073 |
| 6 | C ₃₄ H ₅₀ N ₂ O ₇ | -1961.9761 | -1961.1218 | -1961.2611 | 3.0675 | 398.7220 |
| 7 | C ₂₅ H ₂₄ N ₂ O ₇ | -1603.3000 | -1602.8084 | -1602.9086 | 4.6541 | 294.5400 |

Table 4. Energy (eV) of HOMO, LUMO, energy gap, hardness and softness, chemical potential, electronegativity, and electrophilicity of analogs.

| Entry | ϵ HOMO | ϵ LUMO | Gap | Hardness | Softness | chemical potential | electronegativity | electrophilicity |
|-------|-----------------|-----------------|---------|----------|----------|--------------------|-------------------|------------------|
| 1 | -6.55619 | -0.08953 | 6.46666 | 3.23333 | 0.30928 | -3.32286 | 3.32286 | 1.70743 |
| 2 | -6.53088 | -0.10368 | 6.42720 | 3.21360 | 0.31118 | -3.31728 | 3.31728 | 1.71215 |
| 3 | -6.52408 | -0.08109 | 6.44299 | 3.22149 | 0.31042 | -3.30258 | 3.30258 | 1.69286 |
| 4 | -6.50176 | -0.27647 | 6.22529 | 3.11264 | 0.32127 | -3.38912 | 3.38912 | 1.84507 |
| 5 | -6.68055 | -0.32872 | 6.35183 | 3.17591 | 0.31487 | -3.50463 | 3.50463 | 1.93369 |
| 6 | -6.70857 | -0.10449 | 6.60408 | 3.30204 | 0.30284 | -3.40653 | 3.40653 | 1.75717 |
| 7 | -6.53415 | -0.11919 | 6.41496 | 3.20748 | 0.31177 | -3.32667 | 3.32667 | 1.72514 |

also showed the highest HOMO-LUMO gap and hardness, indicating that the molecule is more reactive than other compounds, according to Pearson *et al.* [49]. In **Figure 1**, the LUMO plot of compound **6** shows that the electrons were localized on the upper part of the thymine ring, while the HOMO plot shows that the electrons were localized at the modified acylating group regions only.

3.4. Molecular Electrostatic Potential (MEP)

The molecular electrostatic potential (MEP) is widely used as a reactivity map displaying the most likely region for electrophilic and nucleophilic attack of charged point-like reagents on organic molecules [50] [51]. It helps to interpret biological recognition processes and hydrogen bonding interactions. The MEP counter map provides a simple way to predict how different geometries could interact. The MEPs of thymidine derivatives (**2** to **7**) are obtained based on the DFT model with the basis set 6 - 31 G (d, p) optimized result and shown in **Figure 2**. The importance of MEP lies in the fact that it simultaneously displays a molecular size and shape as well as positive, negative and neutral electrostatic potential regions in terms of color grading and is very useful in research on molecular structures with physicochemical property relationships. The molecular

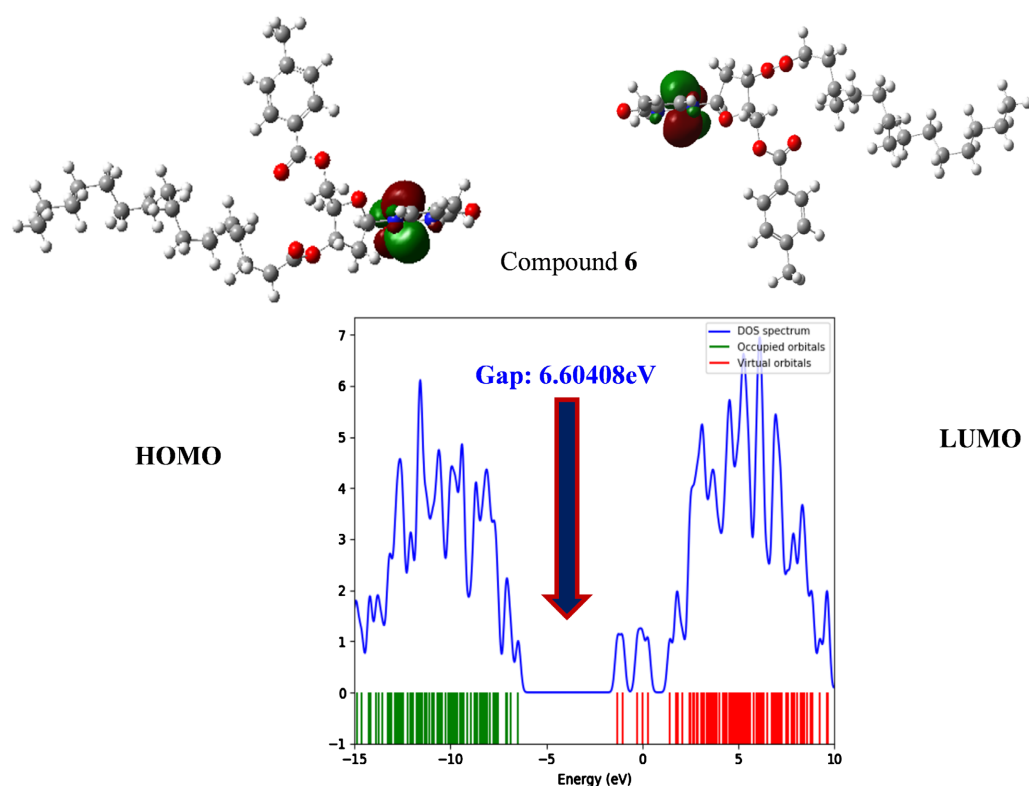


Figure 1. Molecular orbital distribution plots of HOMO and LUMO in the ground state of derivative **6** and DOS diagram.

electrostatic potential (MEP) was calculated to forecast the reactive sites for electrophilic and nucleophilic attack of the optimized structure of thymidine derivatives (**2** - **7**). The different values of electrostatic potential are represented by different colors. Potential increases in the order red < orange < yellow < green < blue. Red represents the maximum negative area, which shows a favorable site for electrophilic attack, blue indicates the maximum positive area favorable for nucleophilic attack, and green represents the zero potential areas.

3.5. Pharmacokinetic Prediction

For predicting the pharmacokinetic properties of drug/drug-like compounds from their structures, ADMET Predictor, a designed computer program, can be used. A drug/drug-like compound has to satisfy the “Rule of Five” [52], which is a well-known parameter to examine whether it can be taken as a drug or not [53]. To analyze whether the modified compounds produce any toxicity or altered pharmacokinetic profile, the admetSAR server was utilized [54] [55]. Different pharmacokinetic and pharmacodynamic parameters, such as human intestinal absorption [56], blood-brain barrier [57], cytochrome P450 inhibition [58], human ether-a-go-go-related gene inhibition [59], acute oral toxicity, rat acute toxicity [60] and aqueous solubility [61], were considered. The results are summarized in **Table 5**. Inhibitory features of hERG can lead to long QT syndrome [62], which is why further investigation is needed. All the compounds

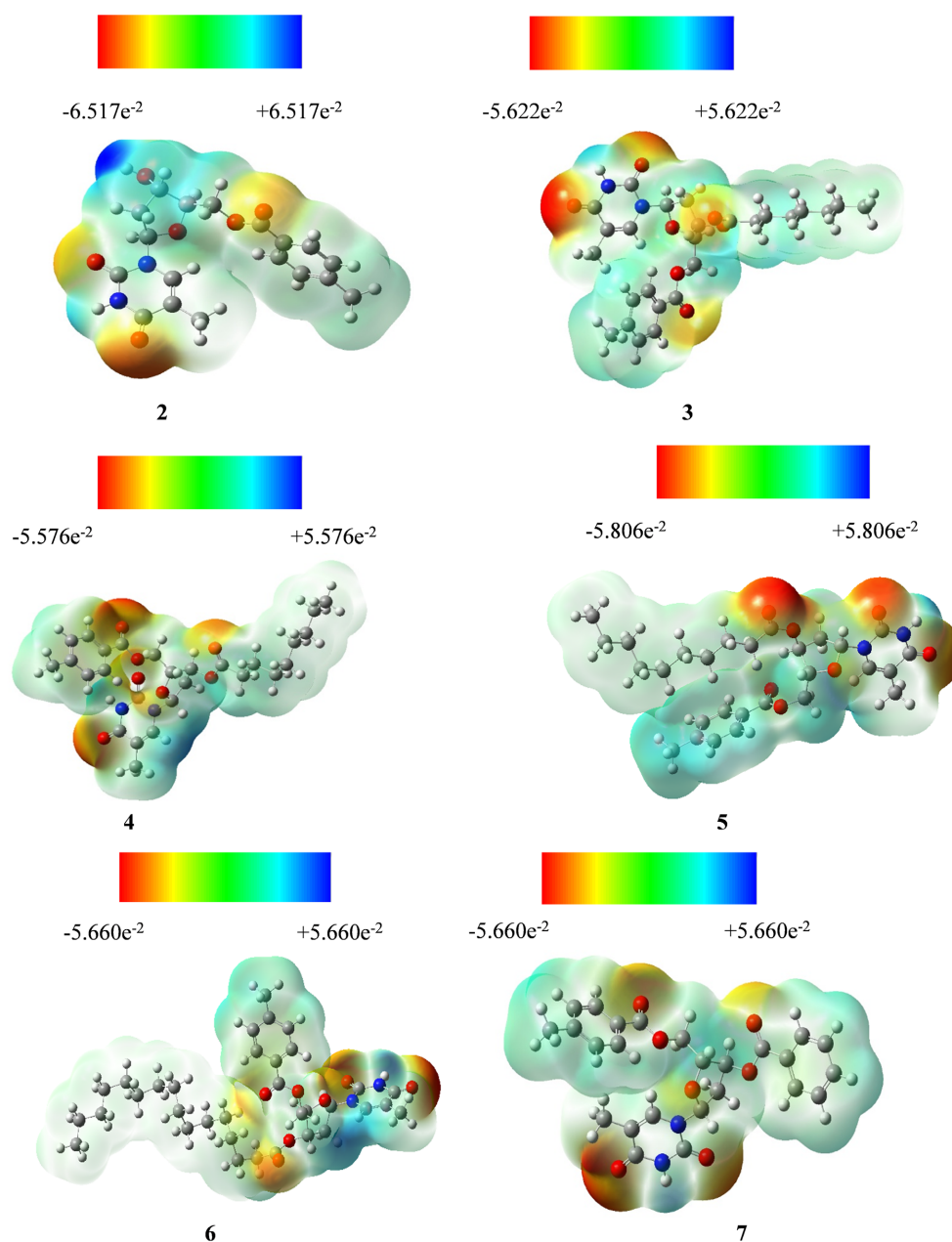


Figure 2. Molecular electrostatic potential map of thymidine derivatives.

were within the acceptable range. Hence, we can say that all the compounds possess a good pharmacokinetic profile.

Lipinski's "rule of five" is a set of guidelines used to evaluate the drug-likeness of potential compounds based on molecular properties that influence their absorption and permeability [63]. **Table 6** shows that only analog (6) violated the rule of five in two cases ($MW > 500$, $MLOGP > 4.15$), indicating the good bio-availability of thymidine analogs.

3.6. Molecular Docking Studies and Ligand–Protein Interactions

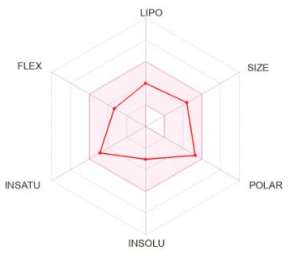
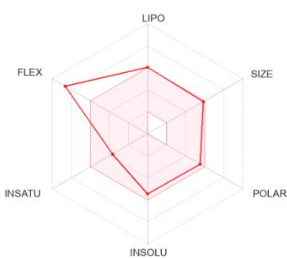
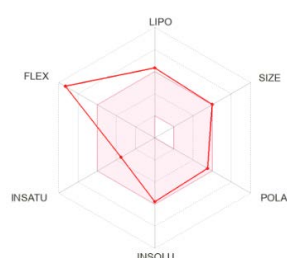
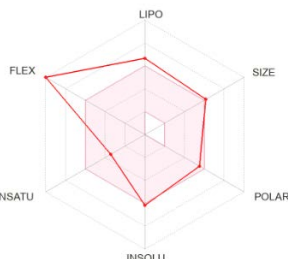
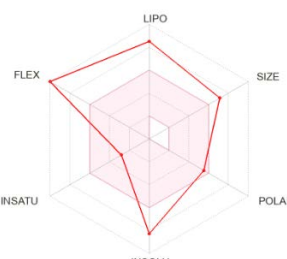
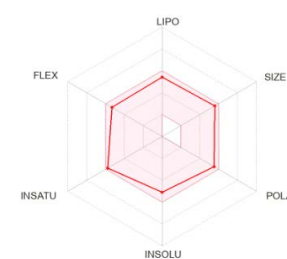
In the field of molecular modeling, molecular docking is a technique that is

Table 5. Selected pharmacokinetic parameters of thymidine and its designed analogs.

| Entry | BBB | Human Intestinal absorption | P-glycogen inhibitor | CYP2C19 inhibitor | hERG | Acute oral toxicity | Aqueous solubility LogS | Rat acute toxicity LD ₅₀ mol/kg |
|-------|---------|-----------------------------|----------------------|-------------------|------------|---------------------|-------------------------|--|
| 1 | +0.5902 | +0.9710 | NI (0.9128) | NI (0.9479) | I (0.9358) | III (0.4665) | 2.08 | 1.870 |
| 2 | -0.6568 | +0.9004 | NI (0.6984) | NI (0.8216) | I (0.9707) | III (0.6016) | -3.15 | 2.017 |
| 3 | +0.8789 | +0.9839 | I (0.7360) | I (0.6571) | I (0.9240) | III (0.6849) | -4.25 | 2.512 |
| 4 | +0.8000 | +0.9613 | I (0.8787) | I (0.6571) | I (0.8923) | III (0.6849) | -4.25 | 3.010 |
| 5 | +0.8356 | +0.8570 | I (0.8789) | I (0.6571) | I (0.9001) | III (0.6849) | -4.25 | 2.996 |
| 6 | +0.8000 | +0.9613 | I (0.8191) | I (0.6970) | I (0.8265) | III (0.6849) | -4.00 | 2.961 |
| 7 | +0.7500 | +0.8961 | NI (0.5403) | I (0.6800) | I (0.9389) | III (0.6612) | -3.50 | 2.129 |

+ = Positive, I = Inhibitor, NI = Non-Inhibitor, III = Category III includes compounds with LD₅₀ greater than 500 mg/kg but less than 5000 mg/kg.

Table 6. Prediction of the drug-likeness properties of thymidine analogs.

| Drug | 02 | 03 | 04 |
|--|---|--|---|
| MW g/mol | 360.36 | 486.56 | 500.58 |
| TPSA (Å ²) | 110.62 | 116.69 | 116.69 |
| (Consensus Log <i>P</i> _{o/w}) | 1.42 | 4.01 | 4.37 |
| Lipinski rule | Yes | Yes | Yes |
| Bioactivity radar charts |  |  |  |
| Drug | 05 | 06 | 07 |
| MW g/mol | 514.61 | 598.77 | 464.47 |
| TPSA (Å ²) | 116.69 | 116.69 | 116.69 |
| (Consensus Log <i>P</i> _{o/w}) | 4.78 | 6.93 | 3.10 |
| Lipinski rule | Yes | No | Yes |
| Bioactivity radar charts |  |  |  |

TPSA-Topological polar surface area.

widely employed to investigate in-depth the interactions between a ligand and receptor and to determine the favored orientation of this ligand to a target receptor. In fact, to determine the preferred receptor for thymidine ligands, we used two different receptors (PDB: 1IYL and 2Y7L). These crystal structures of *C. albicans* were extracted from the Protein Data Bank. Notably, the *Candida albicans* protein was used in this investigation, as reported by S. Bouamrane *et al.*, 2022 and S. J. Dabade *et al.*, 2021 [64] [65]. The spike protein was selected primarily because of its important role in viral infection and pathogenicity. The protein and ligands were submitted to the Vina wizard for docking with the largest box size possible. RMSD (root mean square deviation) is employed for validating docking scores, offering a measure of accuracy in molecular docking predictions. Lower RMSD values indicate better agreement between predicted and actual binding configurations. Before undertaking the molecular docking calculation, the three receptors of interest were readied by eliminating water molecules and minimizing all nonprotein elements and energy. The protein and ligands were submitted to the Vina wizard for docking, and the grid box was maintained at 54.8087, 56.2807 and 67.6774 Å for 1IYL and 42.8078, 76.8638 and 52.5086 Å for 2Y7L along the X, Y, and Z axes, respectively. The analysis revealed that thymidine (**1**), which was found to be active in antibacterial and antifungal tests, exhibited binding affinities of -6.5 and -6.1 kcal·mol⁻¹ for both protease proteins. The binding affinities of its derivatives (**2** - **7**) were approximately -8.7 to -11.2 kcal·mol⁻¹ for 1IYL and (-8.1 to -9.7) for 2Y7L (**Table 7**). We compared the current antifungal drugs fluconazole and voriconazole with our synthesized thymidine analogs. As shown in **Table 7**, derivative **7** showed

Table 7. Binding affinities (kcal/mol) of thymidine and its derivatives.

| Entry | Main protease 1IYL | | | | Main protease 2Y7L | | | |
|--------------|--------------------|--------------|------------------------|---------------------------|--------------------|--------------|------------------------|------------------------|
| | Binding affinity | H-bond (no.) | Hydrophobic bond (no.) | Interaction type | Binding affinity | H-bond (no.) | Hydrophobic bond (no.) | Interaction type |
| 1 | -6.5 | 5 | 1 | H, PS | -6.1 | - | 1 | PPT |
| 2 | -8.8 | 4 | 7 | H, PS, PPT, PA | -9.0 | - | 6 | PPS, PA |
| 3 | -9.8 | 2 | 15 | H, C, PS, PPS, PPT, A, PA | -8.6 | 3 | 10 | H, C, PS, A, PA |
| 4 | -9.7 | 1 | 14 | PS, PPS, PPT, A, PA | -9.3 | 3 | 12 | H, C, PS, PPS, A, PA |
| 5 | -9.2 | - | 11 | PS, PPT, A, PA | -8.1 | 3 | 7 | H, PS, A, PA |
| 6 | -8.7 | 1 | 13 | H, PS, PPS, PPT, A, PA | -8.5 | - | 14 | A |
| 7 | -11.2 | 1 | 11 | H, PS, PPS, PPT, A, PA | -9.7 | - | 8 | PS, PPS, A, PA |
| Fluconazole | -7.9 | 5 | 6 | H, C, PPT, PA | -7.0 | 4 | 4 | H, C, PS, PPS, PA, PPT |
| Voriconazole | -8.3 | 5 | 8 | H, C, PPT, PPS, PA | -7.7 | 3 | 4 | H, C, PPS, PA |

H = Conventional hydrogen bond; C = Carbon-hydrogen bond; A= alkyl; PA = Pi-alkyl; PPS = Pi-Pi stacked; PS = Pi-Sigma; PPT = Pi-Pi T-shaped.

the highest binding affinities compared to the parent compound in the main protease 1IYL. The parent molecule thymidine exhibited interactions with the main protease 1IYL and its residues LYS317, SER318, SER313, GLU309 and VAL316 as well as a sharp interaction within a closer bond distance (1.84865) as a hydrogen bond due to its presence of an oxygen atom in the molecule and a nonbonding interaction with residue THR271 due to the presence of a nitrogen atom (Table 8 and Figure 3). Compounds 3 and 4 both have octanoyl and nonanoyl chloride in their structure, which provides a high gathering of electrons in the molecule and indicates a higher binding score and a higher number of nonbonding interactions. For compound (7), the binding sites were mainly located in a hydrophobic cleft bordered by the amino acid residues PHE339, PHE117, TYR225, PHE339, TYR354, PHE240 and HIS227. There are two hydrogen bond contacts with two different amino acids: TYR225, with a sharp interaction within a closer bond distance (1.80472), and LEU451 (Figure 4). Compound (7) had a *p*-toluoyl chloride and benzoyl chloride aromatic ring substituent in the structure, providing a high gathering of electrons in the molecule and indicating that the highest binding score and nonbonding interactions for the hydrogen bond oxygen atom may be responsible. These results indicated that modification of the –OH group along with a long aliphatic chain/aromatic ring molecule increased the binding affinity, while the addition of hetero groups such as Cl/F caused some fluctuations in binding affinities; however, modification with halogenated aromatic rings also increased the binding affinity. Nonbonding interactions are often used to predict the shape and behavior of molecules. Among all the nonbonding interactions, CH/O, CH/ π , NH/ π , OH/ π , and CH/N, CH/O is the highest observed interaction found in protein-ligand docking.

As shown in Table 7, derivatives (7) showed the highest binding affinities compared to the parent compound in the main protease 2Y7L. For compound (7), there were no hydrogen bonds in contact with any residue, but for nonbonding interactions (contact residues VAL16, VAL161, TYR21, TYR297), compound (7) had a *p*-toluoyl chloride and benzoyl chloride aromatic ring substituent in the structure, providing a high gathering of electrons in the molecule and indicating the highest binding score. In addition, compound (2) has a *p*-toluoyl group, and compound (4) has a nonanoyl group in its structure. For compound (4), the binding sites were mainly located in a hydrophobic cleft bordered by the amino acid residues TRP294, VAL161, ILE167 and TYR166. There are two hydrogen bond contacts with two different amino acids: SER170 and VAL22 (Figure 5). Compound (4) has a nonanoyl chloride and aromatic ring in the structure, providing a high gathering of electrons in the molecule and indicating that the highest binding score and nonbonding interactions and for the hydrogen bond oxygen atom may be responsible. These results indicated that modification of the –OH group along with a long aliphatic chain/aromatic ring molecule increased the binding affinity, while the addition of hetero groups such as Cl/F caused some fluctuations in binding affinities; however, modification with halogenated aromatic rings also increased the binding affinity. Nonbonding

Table 8. Nonbonding interactions of derivatives with the amino acid residue thymidine and its derivatives.

| Entry | Main protease 1IYL | | | | Entry | Main protease 2Y7L | | | |
|-------|--------------------|--------------|------------------|--------------|-------|--------------------|--------------|------------------|--------------|
| | Hydrogen Bond | | Hydrophobic Bond | | | Hydrogen Bond | | Hydrophobic Bond | |
| | Residues | Distance (Å) | Residues | Distance (Å) | | Residues | Distance (Å) | Residues | Distance (Å) |
| 1 | LYS317 | 2.23039 | THR271 | 3.69806 | 1 | - | - | TYR23 | 5.09622 |
| | SER318 | 1.84865 | | | 2 | | | TRP294 | 4.3049 |
| | SER313 | 3.52643 | | | | | | TYR21 | 4.54444 |
| | GLU309 | 2.24097 | | | | | | | |
| 2 | TYR225 | 2.34517 | TYR225 | 4.71035 | | | | TRP294 | 5.15088 |
| | TYR335 | 2.63869 | PHE339 | 4.95741 | | | | TRP295 | 4.8688 |
| | LEU451 | 3.76317 | TYR354 | 4.98797 | 3 | TRP295 | 1.93982 | VAL22 | 3.41107 |
| | TYR354 | 3.18967 | HIS227 | 4.82301 | | TRP295 | 2.17863 | VAL161 | 3.63147 |
| 3 | | | PHE339 | 4.97855 | | | | VAL161 | 5.22052 |
| | ASN392 | 2.50151 | TYR225 | 3.97387 | | | | TYR23 | 5.22398 |
| | TYR225 | 3.6956 | PHE240 | 4.1921 | | | | PHE225 | 5.40655 |
| | | | PHE115 | 4.93228 | | | | TYR297 | 3.41107 |
| 4 | | | PHE339 | 5.05988 | 4 | SER170 | 2.74323 | TRP294 | 5.96634 |
| | | | TYR354 | 5.084 | | VAL22 | 3.367 | TRP294 | 4.35596 |
| | LEU451 | 3.62004 | LEU394 | 3.78415 | | | | VAL161 | 3.65579 |
| | | | PHE117 | 5.77363 | | | | VAL161 | 5.39745 |
| 5 | | | TYR225 | 4.91492 | | | | ILE167 | 4.88157 |
| | | | TYR354 | 5.08986 | | | | TYR166 | 5.31109 |
| | | | PHE115 | 3.66661 | 5 | ILE167 | 3.23925 | TRP294 | 4.83727 |
| | | | TYR225 | 5.24048 | | | | VAL22 | 5.44841 |
| 6 | | | VAL108 | 5.0892 | | | | TYR21 | 5.12941 |
| | TYR225 | 2.16459 | PHE240 | 4.64152 | 6 | | | TYR23 | 4.77561 |
| | | | PHE115 | 5.273 | | | | VAL19 | 4.43868 |
| | | | PHE339 | 4.77004 | | | | VAL22 | 5.18635 |
| 7 | | | LEU394 | 3.98431 | | | | PRO29 | 4.34096 |
| | TYR225 | 1.80472 | PHE339 | 5.38132 | 7 | | | VAL16 | 3.75531 |
| | LEU451 | 3.69646 | PHE117 | 5.05935 | | | | VAL161 | 3.9627 |
| | | | TYR225 | 5.22236 | | | | TYR21 | 5.26821 |
| | | | PHE339 | 4.68098 | | | | TYR297 | 4.94294 |
| | | | TYR354 | 5.11543 | | | | | |
| | | PHE240 | 4.51499 | | | | | | |

Continued

| | | | | | | | | | |
|--------------|--------|---------|--------|---------|--------------|--------|---------|--------|---------|
| | | | HIS227 | 4.44495 | | | | | |
| Fluconazole | TYR225 | 2.11774 | PHE240 | 3.89271 | Fluconazole | THR168 | 2.44774 | TRP294 | 4.36894 |
| | ASN392 | 2.89688 | PHE115 | 5.05978 | | THR168 | 3.0121 | | |
| | HIS227 | 3.32242 | PHE339 | 5.28076 | | ILE167 | 3.68018 | | |
| | TYR225 | 2.87209 | | | Voriconazole | TRP295 | 3.06867 | TRP294 | 5.66495 |
| Voriconazole | THR211 | 2.93309 | LEU451 | 3.69505 | | TRP294 | 3.03524 | TRP294 | 4.31418 |
| | | | PHE117 | 4.33105 | | RP295 | 5.66495 | | |
| | | | TYR225 | 5.17445 | | THR293 | 4.31418 | | |

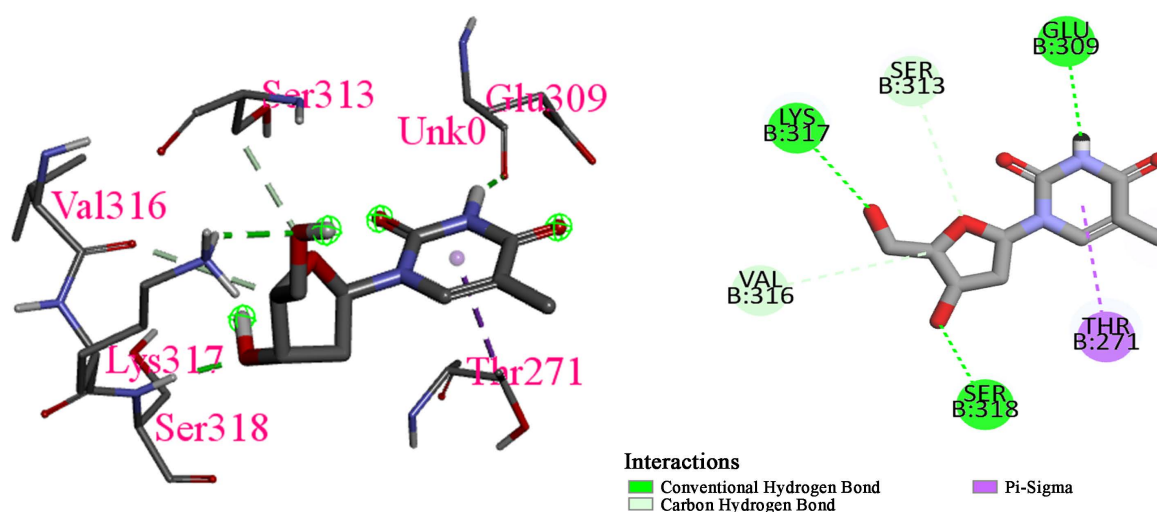


Figure 3. Nonbonding interactions of thymidine with the active site of 1IYL performed by Discovery Studio.

interactions are often used to predict the shape and behavior of molecules (Figure 5).

Although the blind docking studies revealed that all the molecules can act as potential antifungal agents, from the estimated free energy of binding values, we can infer that derivative 7, with the highest negative minimum binding energy values of -11.2 and -9.7 kcal/mol among all the studied compounds, can be the best possible antifungal inhibitor.

4. Conclusion

This research aims to bridge the gap between theoretical and applied aspects of thymidine derivatives by utilizing density functional theory (DFT) for chemical reactivity descriptors. This information is crucial for predicting and interpreting the compounds' behavior in various chemical reactions, offering insights into their reactivity and potential applications. Analysis of various reactivity parameters indicated that these compounds exhibit moderate reactivity. Furthermore, the PASS prediction tool suggested that the derivatives (1-7) possess potential antiviral, antimicrobial and anticarcinogenic properties, and it was revealed that

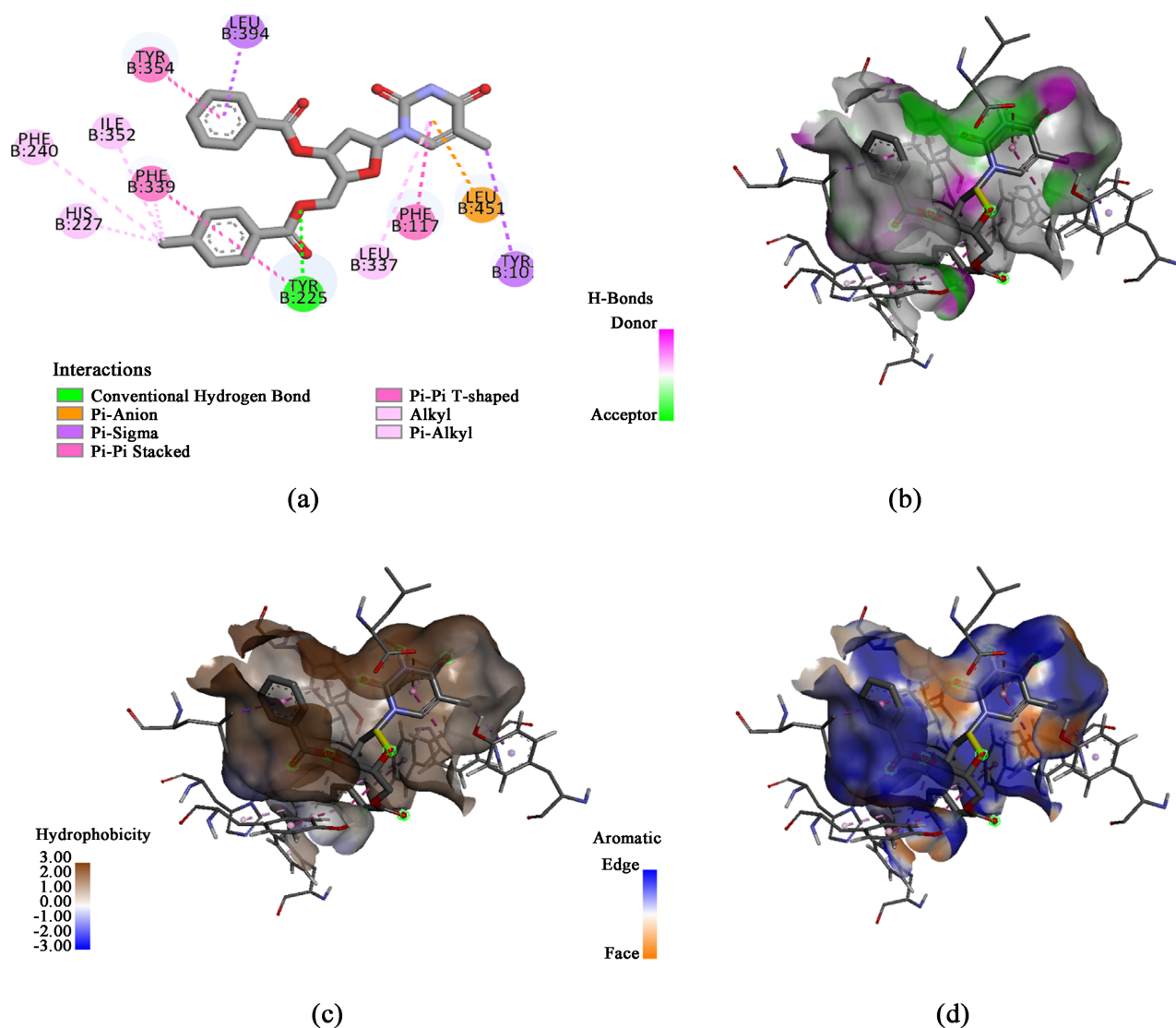


Figure 4. (a) Nonbonding interactions of compounds (7) with the active site of 1IYL, (b) hydrogen bonds, (c) hydrophobicity and (d) aromaticity were performed by Discovery Studio.

compounds were more active against antiviral activity. The moderate predicted biological potential of these compounds may be attributed to a larger HOMO-LUMO gap and hence greater stability. The color-coded representation of molecular electrostatic potential (MEP) aids in correlating molecular structure with physicochemical properties, making it a valuable tool for researchers. The pharmacokinetics of thymidine derivatives are essential for understanding their absorption, distribution, metabolism, and excretion in biological systems, predicting their bioavailability and potential therapeutic efficacy. The results suggest that all the compounds were within the acceptable range, and from the bioactivity radar chart, all compounds followed the Lipinski rule except compound 6. Molecular docking studies help assess the interaction between thymidine derivatives and specific biological targets, providing insights into their binding affinity and potential therapeutic applications. Molecular docking simulations were conducted

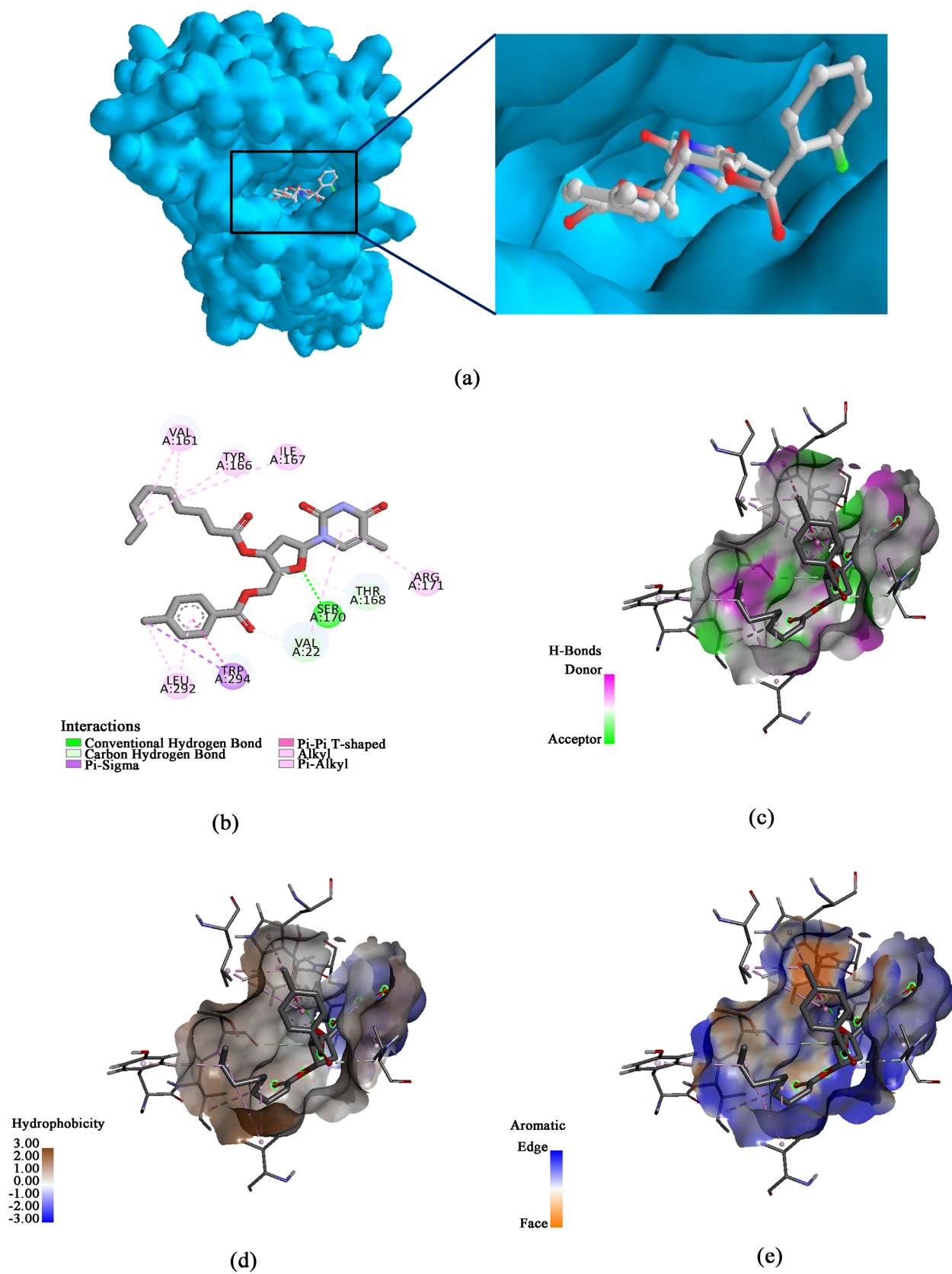


Figure 5. (a) Docked pose of compound **4** with 2Y7L; (b) Nonbonding interactions of compound **4** with the active site of 2Y7L; (c) Hydrogen bonds; (d) Hydrophobicity; (e) Aromaticity were performed by Discovery Studio.

against *C. albicans* (PDB: 1IYL and 2Y7L) to evaluate their antibacterial activity. Notably, compound **7** demonstrated stronger binding affinities toward 1IYL and 2Y7L than the other compounds. However, it is important to note that these compounds may not exhibit the same level of therapeutic efficacy as fluconazole and voriconazole, which are established medications for *C. albicans*. These findings enhance the prospects of these derivatives as potential antifungal agents, paving the way for further experimental investigations and drug development efforts. In summary, this research aims to provide valuable information for researchers in fields such as medicinal chemistry, drug design, and computational biology. The insights gained from this study could contribute to the development of new compounds with enhanced pharmacological properties and potential therapeutic applications.

Acknowledgments

This work was supported by the Japan Society for the Promotion of Science (JSPS, 19K06239 to Yasuhiro Ozeki).

Conflicts of Interest

The authors declare no conflicts of interest regarding the publication of this paper.

References

- [1] Mahmoud, S., Hasabelnaby, S., Hammad, S.F. and Sakr, T.M. (2018) Antiviral Nucleoside and Nucleotide Analogs: A Review. *Journal of Advanced Pharmacy Research*, **2**, 73-88. <https://doi.org/10.21608/aprh.2018.5829>
- [2] De Clercq, E. and Li, G. (2016) Approved Antiviral Drugs over the Past 50 Years. *Clinical Microbiology Reviews*, **29**, 695-747. <https://doi.org/10.1128/CMR.00102-15>
- [3] Guinan, M., Benckendorff, C., Smith, M. and Miller, G.J. (2020) Recent Advances in the Chemical Synthesis and Evaluation of Anticancer Nucleoside Analogs. *Molecules*, **25**, Article 2050. <https://doi.org/10.3390/molecules25092050>
- [4] Eyer, L., Nencka, R., Huvarová, I., Palus, M., Joao Alves, M., Gould, E.A., De Clercq, E. and Růžek, D. (2016) Nucleoside Inhibitors of Zika Virus. *Journal of Infectious Diseases*, **214**, 707-711. <https://doi.org/10.1093/infdis/jjw226>
- [5] Hamuy, R. and Berman, B. (1998) Topical Antiviral Agents for Herpes Simplex Virus Infections. *Drugs Today*, **34**, 1013-1025. <https://doi.org/10.1358/dot.1998.34.12.487486>
- [6] Kawsar, S.M.A., Islam, M., Jesmin, S., Manchur, M.A., Hasan, I. and Rajia, S. (2018) Evaluation of the Antimicrobial Activity and Cytotoxic Effect of Some Uridine Derivatives. *International Journal of Biosciences*, **12**, 211-219.
- [7] Kawsar, S.M.A., Hamida, A.A., Sheikh, A.U., Hossain, M.K., Shagir, A.C., Sanaulah, A.F.M., Manchur, M.A., Imtiaz, H., Ogawa, Y., Fujii, Y., Koide, Y. and Ozeki, Y. (2015) Chemically Modified Uridine Molecules Incorporating Acyl Residues to Enhance Antibacterial and Cytotoxic Activities. *International Journal of Organic Chemistry*, **5**, 232-245. <https://doi.org/10.4236/ijoc.2015.54023>
- [8] Kawsar, S.M.A., Hasan, T., Chowdhury, S.A., Islam, M.M., Hossain, M.K. and Mansur, M.A. (2013) Synthesis, Spectroscopic Characterization, and *in vitro* Antibac-

terial Screening of Some D-Glucose Derivatives. *International Journal of Pure and Applied Chemistry*, **8**, 125-135.

- [9] Kawsar, S.M.A., Matsumoto, R., Fujii, Y., Matsuoka, H., Masuda, N., Iwahara, C., Yasumitsu, H., Kanaly, R.A., Sugawara, S., Hosono, M., Nitta, K., Ishizaki, N., Dogasaki, C., Hamako, J., Matsui, T. and Ozeki, Y. (2011) Cytotoxicity and Glycan-Binding Profile of α -D-Galactose-Binding Lectin from the Eggs of a Japanese Sea Hare (*Aplysia kurodai*). *The Protein Journal*, **30**, 509-519. <https://doi.org/10.1007/s10930-011-9356-7>
- [10] Shagir, A.C., Bhuiyan, M.M.R., Ozeki, Y. and Kawsar, S.M.A. (2016) Simple and Rapid Synthesis of Some Nucleoside Derivatives: Structural and spectral Characterization. *Current Chemistry Letters*, **5**, 83-92. <https://doi.org/10.5267/j.ccl.2015.12.001>
- [11] Arifuzzaman, M., Islam, M.M., Rahman, M.M., Mohammad, A.R. and Kawsar, S.M.A. (2018) An Efficient Approach to the Synthesis of Thymidine Derivatives Containing Various Acyl Groups: Characterization and Antibacterial Activities. *Acta Pharmaceutica Scientia*, **56**, 7-22. <https://doi.org/10.23893/1307-2080.APS.05622>
- [12] Maowa, J., Alam, A., Rana, K.M., Hosen, A., Dey, S., Hasan, I., Fujii, Y., Ozeki, Y. and Kawsar, S.M.A. (2021) Synthesis, Characterization, Synergistic Antimicrobial Properties, and Molecular Docking of Sugar-Modified Uridine Derivatives. *Ovidius University Annals of Chemistry*, **32**, 6-21. <https://doi.org/10.2478/auoc-2021-0002>
- [13] Sultana, S., Hossain, A., Islam, M. and Kawsar, S.M.A. (2024) Antifungal Potential of Mannopyranoside Derivatives through Computational and Molecular Docking Studies against *Candida albicans* I1YL and 1A19 Proteins. *Current Chemistry Letters*, **13**, 1-14. <https://doi.org/10.5267/j.ccl.2023.9.004>
- [14] Bulbul, M.Z.H., Chowdhury, T.S., Misbah, M.M.H., Ferdous, J., Dey, S., Hasan, I., Fujii, Y., Ozeki, Y. and Kawsar, S.M.A. (2021) Synthesis of a New Series of Pyrimidine Nucleoside Derivatives Bearing Acyl Moieties as Potential Antimicrobial Agents. *Pharmacia*, **68**, 23-34. <https://doi.org/10.3897/pharmacia.68.e56543>
- [15] Mirajul, M.I., Arifuzzaman, M., Monjur, M.R., Atiar, M.R. and Kawsar, S.M.A. (2019) Novel Methyl 4, 6-O-Benzylidene- α -D-Glucopyranoside Derivatives: Synthesis, Structural Characterization, and Evaluation of Antibacterial Activities. *Hacetepce Journal of Biology and Chemistry*, **47**, 153-164. <https://doi.org/10.15671/hjbc.622038>
- [16] Devi, S.R., Jesmin, S., Rahman, M., Manchur, M.A., Fujii, Y., Kanaly, R.A., Ozeki, Y. and Kawsar, S.M.A. (2019) Microbial Efficacy and Two-Step Synthesis of Uridine Derivatives with Spectral Characterization. *Acta Pharmaceutica Scientia*, **57**, 47-68. <https://doi.org/10.23893/1307-2080.APS.05704>
- [17] Misbah, M.M.H., Ferdous, J., Bulbul, M.Z.H., Chowdhury, T.S., Dey, S., Hasan, I. and Kawsar, S.M.A. (2020) Evaluation of MIC, MBC, MFC, and Anticancer Activities of Acylated Methyl β -D-Galactopyranoside Esters. *International Journal of Biosciences*, **16**, 299-309.
- [18] Alam, A., Hosen, M.A., Islam, M., Ferdous, J., Fujii, Y., Ozeki, Y. and Kawsar, S.M.A. (2021) Synthesis, Antibacterial, and Cytotoxicity Assessment of Modified Uridine Molecules. *Current Advances in Chemistry and Biochemistry*, **6**, 114-129. <https://doi.org/10.9734/bp/cacb/v6/8670D>
- [19] Farhana, Y., Amin, M.R., Hosen, M.A., Bulbul, M.Z.H., Dey, S. and Kawsar, S.M.A. (2021) Monosaccharide Derivatives: Synthesis, Antimicrobial, PASS, Antiviral, and Molecular Docking Studies against SARS-CoV-2 m^{pro} Inhibitors. *Cellulose Chemistry and Technology*, **55**, 477-499. <https://doi.org/10.35812/CelluloseChemTechnol.2021.55.44>

- [20] Kawsar, S.M.A., Faruk, M.O., Rahman, M.S., Fujii, Y. and Ozeki, Y. (2014) Regioselective Synthesis, Characterization, and Antimicrobial Activities of Some New Monosaccharide Derivatives. *Scientia Pharmaceutica*, **82**, 1-20. <https://doi.org/10.3797/scipharm.1308-03>
- [21] Fujii, Y., Kawsar, S.M.A., Matsumoto, R., Yasumitsu, H., Naoto, I., Dohgasaki, C., Hosono, M., Nitta, K., Hamako, J., Matsui, T. and Ozeki, Y. (2011) A-D-Galactose-Binding Lectin Purified from Coronate Moon Turban, Turbo (Lunella) Coreensis, with a Unique Amino Acid Sequence and the Ability to Recognize Lacto-Series Glycophingolipids. *Comparative Biochemistry and Physiology Part B: Biochemistry and Molecular Biology*, **158**, 30-37. <https://doi.org/10.1016/j.cbpb.2010.09.002>
- [22] Kabir, A.K.M.S., Kawsar, S.M.A., Bhuiyan, M.M.R., Rahman, M.S. and Chowdhury, M.E. (2009) Antimicrobial Screening Studies of Some Derivatives of Methyl α -D-Glucopyranoside. *Pakistan Journal of Scientific and Industrial Research*, **52**, 138-142.
- [23] Kabir, A.K.M.S., Kawsar, S.M.A., Bhuiyan, M.M.R., Rahman, M.S. and Banu, B. (2008) Biological Evaluation of Some Octanoyl Derivatives of Methyl 4, 6-O-Cyclohexylidene- α -D-Glucopyranoside. *Chittagong University Journal of Biological Sciences*, **3**, 53-64. <https://doi.org/10.3329/cujbs.v3i1.13406>
- [24] Kabir, A.K.M.S., Kawsar, S.M.A., Bhuiyan, M.M.R., Islam, M.R. and Rahman, M.S. (2004) Biological Evaluation of Some Mannopyranoside Derivatives. *Bulletin of Pure & Applied Sciences*, **23**, 83-91.
- [25] Islam, S., Hosen, M.A., Ahmad, S., Qamar, M.T.U., Dey, S., Hasan, I., Fujii, Y., Ozeki, Y. and Kawsar, S.M.A. (2022) Synthesis, Antimicrobial, Anticancer Activities, PASS Prediction, Molecular Docking, Molecular Dynamics, and Pharmacokinetic Studies of Designed Methyl α -D-Glucopyranoside Esters. *Journal of Molecular Structure*, **1260**, Article ID: 132761. <https://doi.org/10.1016/j.molstruc.2022.132761>
- [26] Hosen, M.A., Munia, N.S., Al-Ghorbani, M., Baashen, M., Almalki, F.A., Hadda, T.B., Ali, F., Mahmud, S., Saleh, M.A., Laaroussi, H. and Kawsar, S.M.A. (2022) Synthesis, Antimicrobial, Molecular Docking, and Molecular Dynamics Studies of Lauroyl Thymidine Analogs against SARS-CoV-2: POM Study and Identification of the Pharmacophore Sites. *Bioorganic Chemistry*, **125**, Article ID: 105850. <https://doi.org/10.1016/j.bioorg.2022.105850>
- [27] Farhana, Y., Amin, M.R., Hosen, A. and Kawsar, S.M.A. (2021) Bromobenzylation of Methyl α -D-Mannopyranoside: Synthesis and Spectral Characterization. *Journal of Siberian Federal University, Chemistry*, **14**, 171-183. <https://doi.org/10.17516/1998-2836-0226>
- [28] Rana, K.M., Ferdous, J., Hosen, A. and Kawsar, S.M.A. (2020) Ribose Moieties Acylation and Characterization of Some Cytidine Analogs. *Journal of Siberian Federal University, Chemistry*, **13**, 465-478. <https://doi.org/10.17516/1998-2836-0199>
- [29] Frisch, M.J., Trucks, G.W., Schlegel, H.B., Scuseria, G.E., Robb, A., Cheeseman, J.R., Scalmani, G., Barone, V., Mennucci, B., Petersson, G.A., *et al.* (2009) Gaussian 09. Gaussian Inc, Wallingford.
- [30] Tirado-Rives, J. and Jorgensen, W.L. (2008) Performance of B3LYP Density Functional Methods for a Large Set of Organic Molecules. *Journal of Chemical Theory and Computation*, **4**, 297-306. <https://doi.org/10.1021/ct700248k>
- [31] Becke, A.D. (1988) Density-Functional Exchange-Energy Approximation with Correct Asymptotic Behavior. *Physical Review A*, **38**, 3098-3100. <https://doi.org/10.1103/PhysRevA.38.3098>
- [32] Lee, C., Yang, W. and Parr, R.G. (1988) Development of the Colle-Salvetti Correlation-Energy Formula into a Functional of the Electron Density. *Physical Review B*, **37**, 785-789. <https://doi.org/10.1103/PhysRevB.37.785>

- [33] Parr, R.G. (1980) Density Functional Theory of Atoms and Molecules. In: Fukui, K. and Pullman, B., Eds., *Horizons of Quantum Chemistry*, Springer, Dordrecht, 5-15. https://doi.org/10.1007/978-94-009-9027-2_2
- [34] Kumaresan, S., Senthilkumar, V., Stephen, A. and Balakumar, B. (2015) GC-MS Analysis and PASS-Assisted Prediction of Biological Activity Spectra of Extract of *Phomopsis* sp. Isolated from *Andrographis paniculata*. *World Journal of Pharmaceutical Research*, **4**, 1035-1053.
- [35] Kawsar, S.M.A., Kumer, A., Munia, N.S., Hosen, M.A., Chakma, U. and Akash, S. (2022) Chemical Descriptors, PASS, Molecular Docking, Molecular Dynamics and ADMET Predictions of Glucopyranoside Derivatives as Inhibitors to Bacteria and Fungi Growth. *Organic Communications*, **15**, 184-203. <https://doi.org/10.25135/acg.oc.122.2203.2397>
- [36] Kawsar, S.M.A., Hosen, M.A., Chowdhury, T.S., Rana, K.M., Fujii, Y. and Ozeki, Y. (2021) Thermochemical, PASS, Molecular Docking, Drug-Likeness and in Silico ADMET Prediction of Cytidine Derivatives against HIV-1 Reverse Transcriptase. *Revista de Chimie*, **72**, 159-178. <https://doi.org/10.37358/RC.21.3.8446>
- [37] Hosen, M.A., Alam, A., Islam, M., Fujii, Y., Ozeki, Y. and Kawsar, S.M.A. (2021) Geometrical Optimization, PASS Prediction, Molecular Docking, and in Silico ADMET Studies of Thymidine Derivatives against FimH Adhesin of *Escherichia coli*. *Bulgarian Chemical Communications*, **53**, 327-342.
- [38] Alam, A., Hosen, M.A., Hosen, A., Fujii, Y., Ozeki, Y. and Kawsar, S.M.A. (2021) Synthesis, Characterization, and Molecular Docking against a Receptor Protein FimH of *Escherichia coli* (4XO8) of Thymidine Derivatives. *Journal of the Mexican Chemical Society*, **65**, 256-276. <https://doi.org/10.29356/jmcs.v65i2.1464>
- [39] Maowa, J., Hosen, M.A., Alam, A., Rana, K.M., Fujii, Y., Ozeki, Y. and Kawsar, S.M.A. (2021) Pharmacokinetics and Molecular Docking Studies of Uridine Derivatives as SARS-CoV-2 M^{pro} Inhibitors. *Physical Chemistry Research*, **9**, 385-412.
- [40] Sim, F., St-Amant, A., Papai, I. and Salahub, D.R. (1992) Gaussian Density Functional Calculations on Hydrogen-Bonded Systems. *Journal of the American Chemical Society*, **114**, 4391-4400. <https://doi.org/10.1021/ja00037a055>
- [41] Shamsuddin, T., Hosen, M.A., Alam, M.S., Emran, T.B. and Kawsar, S.M.A. (2021) Uridine Derivatives: Antifungal, PASS Outcomes, ADME/T, Drug-Likelihood, Molecular Docking and Binding Energy Calculations. *Medicine Science-International Medical Journal*, **10**, 1373-1386. <https://doi.org/10.5455/medscience.2021.05.175>
- [42] Amin, M.R., Yasmin, F., Dey, S., Mahmud, S., Saleh, M.A., Emran, T.B., Hasan, I., Rajia, S., Ogawa, Y., Fujii, Y., Yamada, M., Ozeki, Y. and Kawsar, S.M.A. (2021) Synthesis, Antimicrobial, Anticancer, PASS, Molecular Docking, Molecular Dynamic Simulations and Pharmacokinetic Predictions of Some Methyl β -D-Galactopyranoside Analogs. *Molecules*, **26**, Article 7016. <https://doi.org/10.3390/molecules26227016>
- [43] Amin, M.R., Yasmin, F., Hosen, M.A., Dey, S., Mahmud, S., Saleh, M.A., Emran, T.B., Hasan, I., Fujii, Y., Yamada, M., Ozeki, Y. and Kawsar, S.M.A. (2021) Methyl β -D-Galactopyranoside Esters as Potential Inhibitors for SARS-CoV-2 Protease Enzyme: Synthesis, Antimicrobial, PASS, Molecular Docking, Molecular Dynamics Simulations and Quantum Computations. *Glycoconjugate Journal*, **39**, 261-290. <https://doi.org/10.1007/s10719-021-10039-3>
- [44] Kawsar, S.M.A., Hosen, M.A., Fujii, Y. and Ozeki, Y. (2020) Thermochemical, DFT, Molecular Docking and Pharmacokinetic Studies of Methyl β -D-Galactopyranoside Esters. *Journal of Computational Chemistry and Molecular Modeling*, **4**, 452-462.

- <https://doi.org/10.25177/JCCMM.4.4.RA.10663>
- [45] Kawsar, S.M.A. and Hosen, M.A. (2020) An Optimization and Pharmacokinetic Studies of Some Thymidine Derivatives. *Turkish Computational and Theoretical Chemistry*, **4**, 59-66. <https://doi.org/10.33435/tcandtc.718807>
- [46] Kawsar, S.M.A. and Kumar, A. (2021) Computational Investigation of Methyl α -D-Glucopyranoside Derivatives as Inhibitors against Bacteria, Fungi, and COVID-19 (SARS-2). *Journal of the Chilean Chemical Society*, **66**, 5206-5214. <https://doi.org/10.4067/S0717-97072021000205206>
- [47] Politzer, P. and Murray, J.S. (1991) Molecular Electrostatic Potentials and Chemical Reactivity. *Reviews in Computational Chemistry*, **2**, 273-312. <https://doi.org/10.1002/9780470125793.ch7>
- [48] Alam, A., Rana, K.M., Hosen, M.A., Dey, S., Bezbaruah, B. and Kawsar, S.M.A. (2022) Modified Thymidine Derivatives as Potential SARS-CoV Inhibitors: An Approach of PASS Prediction, *in vitro* Antimicrobial, Physicochemical, and Molecular Docking Studies. *Physical Chemistry Research*, **10**, 391-409.
- [49] Pearson, R.G. (1988) Absolute Electronegativity and Hardness: Application to Organic Chemistry. *Journal of Organic Chemistry*, **27**, 734-740. <https://doi.org/10.1021/ic00277a030>
- [50] Islam, A.U., Serseg, T., Benarous, K., Ahmmed, F. and Kawsar, S.M.A. (2023) Synthesis, Antimicrobial Activity, Molecular Docking and Pharmacophore Analysis of New Propionyl Mannopyranosides. *Journal of Molecular Structure*, **1292**, Article ID: 135999. <https://doi.org/10.1016/j.molstruc.2023.135999>
- [51] Murray, J.S. and Politzer, P. (2017) Molecular Electrostatic Potentials and Noncovalent Interactions. *WIREs Computational Molecular Science*, **7**, e1326. <https://doi.org/10.1002/wcms.1326>
- [52] Daina, A., Michielin, O. and Zoete, V. (2017) SwissADME: A Free Web Tool to Evaluate Pharmacokinetics, Drug-Likeness and Medicinal Chemistry Friendliness of Small Molecules. *Scientific Reports*, **7**, Article No. 42717. <https://doi.org/10.1038/srep42717>
- [53] Pires, D.E.V., Blundell, T.L. and Ascher, D.B. (2015) pkCSM: Predicting Small-Molecule Pharmacokinetic and Toxicity Properties Using Graph-Based Signatures. *Journal of Medicinal Chemistry*, **58**, 4066-4072. <https://doi.org/10.1021/acs.jmedchem.5b00104>
- [54] Kawsar, S.M.A., Hosen, M.A., El Bakri, Y., Ahmad, S., Affi, S.T. and Goumri-Said, S. (2022) In Silico Approach for Potential Antimicrobial Agents through Antiviral, Molecular Docking, Molecular Dynamics, Pharmacokinetic and Bioactivity Predictions of Galactopyranoside Derivatives. *Arabian Journal of Basic and Applied Sciences*, **29**, 99-112. <https://doi.org/10.1080/25765299.2022.2068275>
- [55] Yang, H., *et al.* (2019) admetSAR 2.0: Web-Service for Prediction and Optimization of Chemical ADMET Properties. *Bioinformatics*, **35**, 1067-1069. <https://doi.org/10.1093/bioinformatics/bty707>
- [56] Shen, J., Cheng, F., Xu, Y., Li, W. and Tang, Y. (2010) Estimation of ADME Properties with Substructure Pattern Recognition. *Journal of Chemical Information and Modeling*, **50**, 1034-1041. <https://doi.org/10.1021/ci100104j>
- [57] Wang, Z., *et al.* (2018) In Silico Prediction of Blood-Brain Barrier Permeability of Compounds by Machine Learning and Resampling Methods. *ChemMedChem*, **13**, 2189-2201. <https://doi.org/10.1002/cmdc.201800533>
- [58] Cheng, F., *et al.* (2011) Classification of Cytochrome P450 Inhibitors and Noninhibitors Using Combined Classifiers. *Journal of Chemical Information and Modeling*, **51**, 996-1011. <https://doi.org/10.1021/ci200028n>

- [59] Sun, L., *et al.* (2015) In Silico Prediction of Chemical Aquatic Toxicity with Chemical Category Approaches and Substructural Alerts. *Toxicology Research*, **4**, 452-463. <https://doi.org/10.1039/C4TX00174E>
- [60] Zhu, H., Martin, T.M., Ye, L., Sedykh, A., Young, D.M. and Tropsha, A. (2009) Quantitative Structure-Activity Relationship Modeling of Rat Acute Toxicity by Oral Exposure. *Chemical Research in Toxicology*, **22**, 1913-1921. <https://doi.org/10.1021/tx900189p>
- [61] Wang, J., Krudy, G., Hou, T., Zhang, W., Holland, G. and Xu, X. (2007) Development of Reliable Aqueous Solubility Models and Their Application in Druglike Analysis. *Journal of Chemical Information and Modeling*, **47**, 1395-1404. <https://doi.org/10.1021/ci700096r>
- [62] Huang, F.D., Chen, J., Lin, M., Keating, M.T. and Sanguinetti, M.C. (2001) Long-QT Syndrome-Associated Missense Mutations in the Pore Helix of the HERG Potassium Channel. *Circulation*, **104**, 1071-1075. <https://doi.org/10.1161/hc3501.093815>
- [63] Lipinski, C.A., Lombardo, F., Dominy, B.W. and Feeney, P.J. (2001) Experimental and Computational Approaches to Estimate Solubility and Permeability in Drug Discovery and Development Settings. *Advanced Drug Delivery Reviews*, **46**, 3-26. [https://doi.org/10.1016/S0169-409X\(00\)00129-0](https://doi.org/10.1016/S0169-409X(00)00129-0)
- [64] Mandloi, D., Dabade, S.J., Bajaj, A.V. and Atre, H. (2020) Molecular Docking and QSAR Studies for Modeling Antifungal Activity of Triazine Analogs against Therapeutic Target NMT of *Candida albicans*. *International Journal of Pharmaceutical Sciences and Drug Research*, **13**, 140-146. <https://doi.org/10.25004/IJPSDR.2021.130204>
- [65] Bouamrane, S., Khaldan, A., Hajji, H., El-Mernissi, R., Maghat, H., Ajana, M.A., Sbai, A., Bouachrine, M. and Bouachrine, M. (2022) 3D-QSAR, Molecular Docking, Molecular Dynamic Simulation, and ADMET Study of Bioactive Compounds against *Candida albicans*. *Moroccan Journal of Chemistry*, **10**, 523-541.